

Toward a Better Air-Assisted Flare Design for Safe and Efficient Operation during Purge Flow Conditions: Designing and Performance Testing

Hayder A. Alhameedi, Joseph D. Smith,* Paul Ani, and Tanner Powley



Cite This: *ACS Omega* 2022, 7, 42793–42800



Read Online

ACCESS |

Metrics & More

Article Recommendations

Supporting Information

ABSTRACT: In this study, a new air-assisted flare tip was designed, built, and tested under different operating conditions. Lacking sufficient energy to mix with air, low waste gas flow rates will lead to incomplete combustion of these gases. This increases pollutant emissions and soot formation which leads to a decline in flare performance. This flare tip design enhances the waste gas mixing energy through implementation of an air jet in a crossflow orientation. This is done by adjusting the exit area of the waste gas exit by injecting a radial jet of air from an inclined slot jet located around the flare tip. This flare tip design also provides protection for the flare tip from high flame temperatures that can damage through convective cooling. Several tests were conducted to assess the new flare tip design with varying waste gas flow rates of 5, 10, 25, and 120 standard liters per minute (SLPM). These tests also considered varying assistant air flow rates. In addition, test results showed high combustion efficiency of the flaring process and significant soot formation suppression. The new flare tip design yielded better flame behavior with respect to the flare tip, caused by the flame stability that prevented the flame from attaching to the flare tip.



1. INTRODUCTION

Flares are considered safety equipment that prevent uncontrolled failures in petrochemical processing facilities. Flares provide an efficient and smokeless discharge point for the waste and relief gases in chemical and petrochemical plants.¹ Flaring involves the combustion of flammable relief gases in an open environment to prevent the release of these waste gases into the atmosphere, which would negatively impact human health and the environment.^{2,3} These flares must reliably operate with high efficiency. Except for intervals of not more than 5 min during a 2 h period, the flare must operate with no visible smoke emissions, according to EPA 40 CFR 60.18.⁴ The combustion efficiency (CE), the mass percentage of waste gases converted into carbon dioxide, and the destruction removal efficiency (DRE), the mass percentage of hydrocarbons that are converted to other products, are the parameters that used to evaluate the flare performance. A flare performance with a combustion efficiency of 96.5 or above is considered “good” performance.⁵ To calculate the CE, the following equation is used:

$$\text{CE \%} = \frac{\text{CO}_2 \text{ concentration in the plume}}{(\text{CO}_2 + \text{CO} + \text{total HC})_{\text{plume}}} \times 100 \quad (1)$$

where CE % is the combustion efficiency (%), “CO₂” is the volume concentration of carbon dioxide in the plume after combustion occurs, “CO” is the volume concentration of

carbon monoxide in the plume after combustion occurs, and “total HC” is the volume concentration of unburned hydrocarbons in the plume after combustion has occurred.⁶ Soot is not included in the CE calculation because, in general, the soot volume fraction is less than 10⁻⁵, which has no significant impact on the CE.

Assist medium (air or steam) is normally used in flares to enhance the combustion efficiency and provide smokeless operation when flaring waste gases. An air-assisted flare uses ambient air as an assist medium to promote “good” mixing, which leads to high CE.⁷ An advantage of using air-assisted flares over steam-assisted flares is the lower cost of using air compared to steam. Also, air-assisted flares are useful in cold climates where steam would condense and freeze and in regions where water is in short supply. However, excessive amounts of air lead to reduced CE due to lower flammability conditions. Another factor that leads to reducing the flare performance is the low waste gas flow rate during “purge flow conditions”. Waste gases in these flow conditions do not have sufficient mixing energy to effectively mix waste gas with the

Received: July 21, 2022

Accepted: November 3, 2022

Published: November 16, 2022



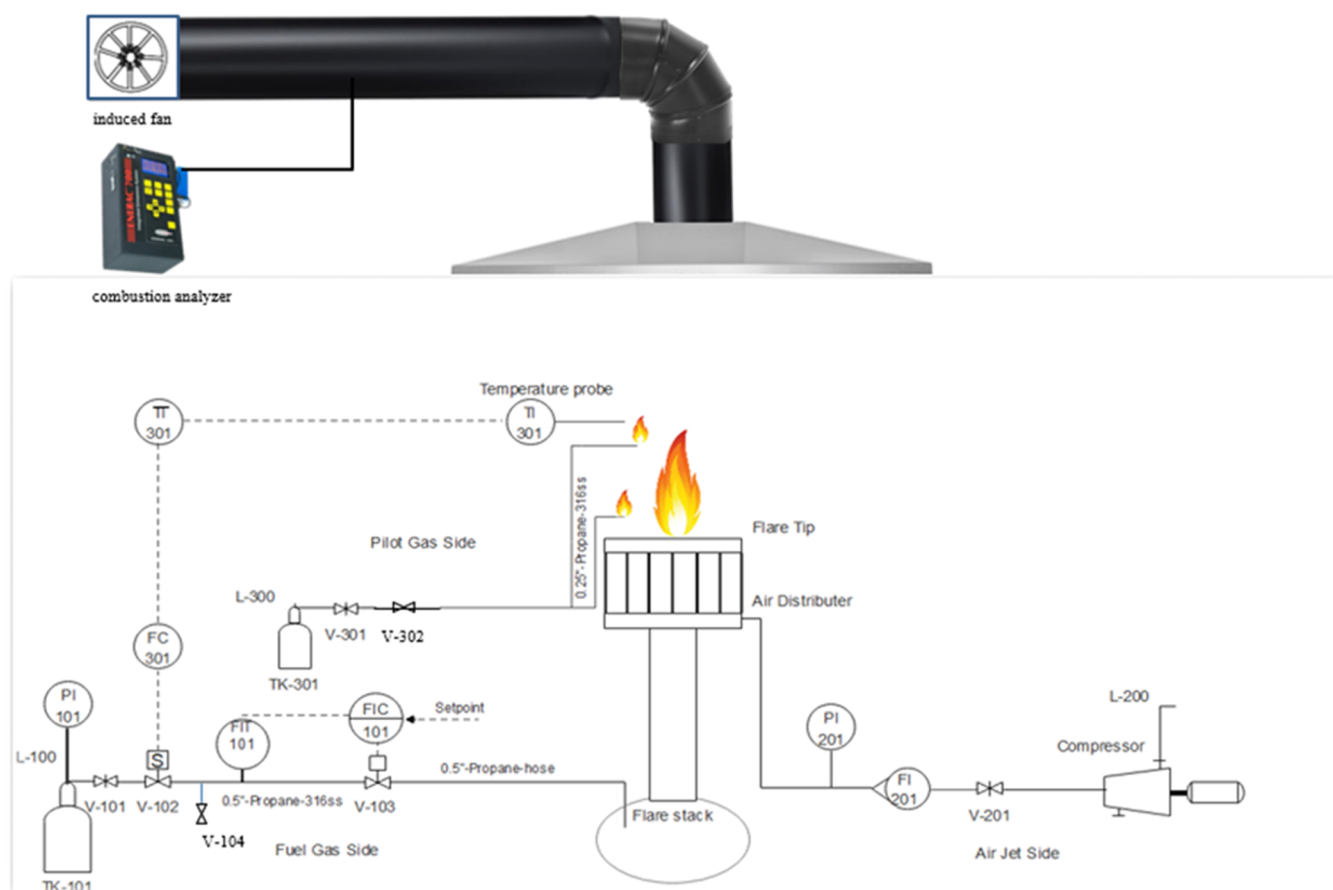


Figure 1. Flare test facility process.

surrounding ambient air. Consequently, this leads to poor mixing in the combustion zone, which causes low CE.⁸

Several previous experimental and theoretical studies have been conducted to investigate the effects of flare assist media,^{7,9–12} waste gas flow rate,^{6,13,14} and other operating factors including waste gases heating value,^{9,15} crosswind velocity,^{16,17} flare head configuration,¹⁰ etc. as relates to the CE aimed at finding the optimum range of each factor to achieve high CE. A brief review of the previous studies related to flare testing under different operating parameters has been conducted. These studies clarify the effect of different flare operating parameters on flare performance. The analysis of previous studies also sets the basis for the present work. A summary of this review is presented in Table S1 (see the Supporting Information).

Bello et al. performed an experimental study to measure and compare emissions from water- and steam-assisted flares for different waste gas mixtures of propane and methane gases. They found that water-assisted flare suppresses soot emissions and decreases NO_x and soot emissions more than steam-assisted flare.¹² Ahsan et al. investigated the effects of air and steam assist on flare CE and pollutant emissions. In their work, a concentric two-circular tubes burner was used to provide coflow of natural gas and assist medium. According to experimental results, combustion efficiency decreases dramatically when the assist media to waste gas mass ratio of 5 and 1.8 for air- and steam-assist flaring operations was used, respectively.¹¹ Zamani et al. studied the impacts of the waste gas composition and flow rate, assistant fluid flow rate, and burner head geometry. They found that combustion efficiency

declined rapidly after some critical flow rates of assistance fluids.¹⁸ However, most of these studies have been done on pilot flares (inner diameter < 6 in.), which differ greatly from industrial scale flares, as discussed by Ahsan et al., who showed that there are differences in the threshold value of the ratio of assistant fluid to waste gas mass flow where the CE decreases.¹¹

The TCEQ2010 Flare Study is considered one of the most important investigations on industrial scale air- and steam-assisted flares. This study examined the effects of several parameters, including low flow rates and the heating values of waste gases, and varying assistant amounts. Among the parameters examined was the amount of assist medium and low flow rate of waste gases. This study concluded that excess air or steam negatively affects flare performance. It also showed that flare efficiency was lower for low flow rates of waste gases.⁶ Other studies have relied on the TCEQ2010 flare study to help quantifying flare performance in terms of various operating conditions.^{14,19–21}

There are several typical air-assisted flare tip geometries that are utilized to provide a smokeless flaring process, such as an external air ring, drilled spider, triangular arm, internal tube, etc. The simplest air-assisted flare tip design is the external air ring design, in which a ring of small pipe to inject air is located around a central pipe or utility flare. This design has a lower capital cost than the other air-assisted flare tip designs. However, these kinds of flares are used to handle large volumes of low-pressure waste. The drilled spider flare tip design has pipes or plates at the tip similar to spider arms that have multiple holes through which gas flows from a riser pipe

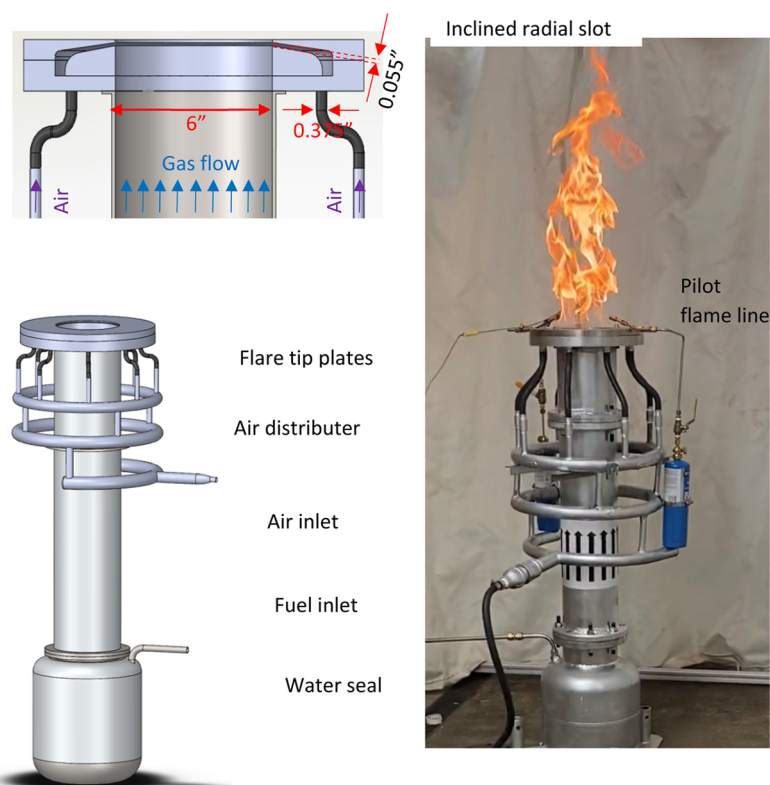


Figure 2. Physical setup.

located in the center of the flare. In this type, air is injected into the flare stack to cause it to flow into the flare tip through the gaps between the spider arms. This can provide the required mixing of flared gas with air at the flare tip. The triangular arm flare tip design is used for the larger volume of flare gases. In this design, flare gases flow through triangular gaps, and air flows through the other triangular gaps between the gas triangular gaps. For the larger amounts of flared gas that are required to be handled, the internal tube flare tip design is used. In this design, a bundle of pipes is used inside a flare tip to allow air to flow through them while gas flows through the gaps between these pipes.²²

Few studies have been conducted to investigate the effects of a flare's design related to flare performance. Al-Fadhly et al. investigated the impact of using different blower configurations on the air-assisted flare emissions. They used four different configurations of fixed and variable, single and dual speed configurations. They found that the variable speed blower configurations achieved lower predicted emissions than the fixed speed blowers of the same size.²³ Mostafayi and Rashidi investigated numerically the effects of splitting industrial flare tip into several branches on the soot formation and NO_x emissions.²⁴ Based on these previous works, it appears a newly designed flare tip is required to overcome the problem of low CE at low flow conditions of waste gases to ensure efficient flaring. Thus, this paper, which is the final part of a series of studies on designing a new air-assisted flare tip, describes the design, construction, and testing of a high-performance air-assisted flare that can efficiently operate under a wide range of flow rates, including purge flow conditions. In the first part of this series of studies, the experimental data required to validate a Computational Fluid Dynamics (CFD) model were collected.⁸ In the second part, the validated CFD model was

used to examine the impact of different design parameters (injection angle, slot height, jet velocity) on the flow field above the flare tip.²⁵ Based on the findings of these studies, the best design parameters were selected and used in this study to build the new flare tip.

2. EXPERIMENTAL SETUP AND METHODOLOGY

2.1. Experimental Setup. The flare facility test setup was designed and built for this work, is presented in Figures 1 and 2. The new flare tip was tested under various operating conditions. Previous studies on flares^{8,25} were conducted to investigate the impact of the radial slot air jet on the crossflow field. The first study was focused on collecting the required experimental data using cold flow conditions for a radial slot air jet injected perpendicularly into air crossflow. The second study was conducted to establish a computational fluid dynamics model (CFD) to evaluate the impacts of different flare design factors on the flow dynamics. These studies have increased our understanding of flare tip operation, which has helped improve its performance.

Test setup considered three sections: the air, fuel (waste gas), and flare. The air section was used to provide the required assistance air for the radial slot jet. This section included an air compressor, pressure gauge regulator, needle valve, rotameter, pressure gauge, and air distributor. All these instruments were connected to the flare tip. The air distributor consisted of two and a half sections of 1-in. diameter pipe followed by a 16-in. section diameter as shown in Figure 2. The inlet pipe for the air distributor was a 0.5-in. diameter pipe fitting attached to the middle of the half-ring pipe section, and the output of this half ring section were two 0.5-in. diameter section and 4-in. length pipes located at the ends of the half ring section. These 0.5-in. pipes formed the entrance to the

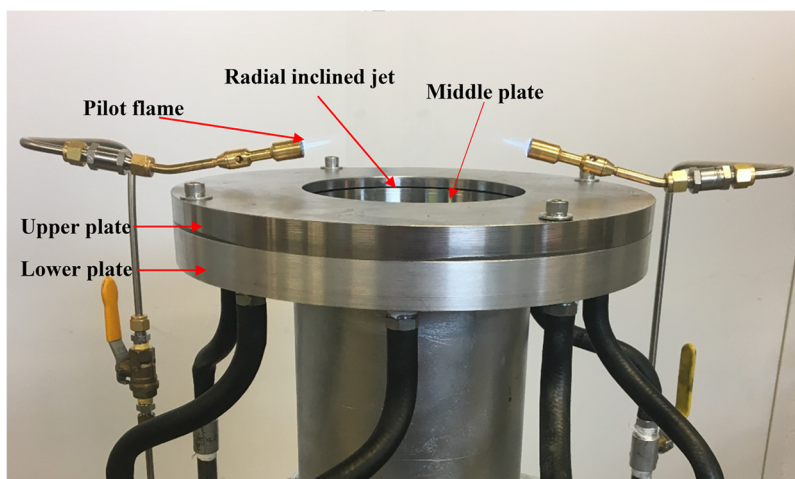


Figure 3. Flare tip and pilot flames.

first ring, which had four 0.5-in. pipes outlets. Also, these four pipes' outlets formed the inlets to the second ring, consisting of eight 0.375-in. diameter pipe fittings on the other end. These eight pipe fittings were connected to eight 0.375-in. diameter flexible hose sections connected to the bottom plate of the slot jet. This distributor design ensured a uniform air flow through all eight entrance ports of the slot jet plates, which provided a uniform flow to the radial slot.

The fuel section provided flare gas from a pressurized gas tank flowing through a water seal to the flare tip. This section consisted of a 100 lb. propane tank with a ball valve shut-off followed by a one-way valve, a solenoid valve, and a mass flow controller. Together, these components fed flare gas to the water seal through a 0.5-in. stainless steel pipe. The main shut-off valve provided a safe way to control the system by simply shutting off the flare gas to prevent propane gas from flowing into the flare system. This section included a nitrogen feed with a needle valve just after the main shut-off valve to allow purging of the flare system after each experiment to ensure no fuel remained in the main feed pipe. The one-way valve prevented the backflow of high-pressure nitrogen into the propane cylinder. The propane tank was located 30 ft. away from the flare setup.

The next section of the flare system consisted of a water seal, flare stack, flare tip, and pilot flame as shown in Figure 2. The water seal was made with a 20-lb gas cylinder partially filled with water prior to each experiment. The water seal added a second layer of safety to the flare system in case the flame flashed back through the flare stack to create a confined space explosion in the system. The flare stack was constructed of three 6-in. diameter pipes of 2.5-in., 24-in., and 10-in. lengths, as shown in Figure 2. These pipes were connected in series to the water seal outlet by flanges. The upper pipe was connected to the flare tip.

The flare tip was constructed of two flat 304 stainless steel annular plates and an aluminum annular plate as shown in Figure 3. The inlet air passage to create the slot jet was made using these flat annular plates, each with different sizes and configurations. The bottom annular aluminum plate had dimensions of a 6-in. inner and a 12-in. outer diameter, respectively. The second annular plate (middle), attached to the bottom plate, had a 6-in. inner and a 10-in. outer diameter, respectively. The middle plate was a 0.5-in.-thick perimeter that sloped to the inner diameter. The upper plate was a 6-in.

inner and a 12-in. outer diameter, respectively. The upper plate surface was flat, while the lower surface had the same slope as the middle plate. The sloped surfaces of the middle and upper plates provided the gap that formed an inclined radial slot to feed air uniformly into the flare stack. These three plates were attached to the flare stack by four screws through the bottom plate. Two premixed pilot flames (see Figure 3) provided a continuous ignition source for the flare gas to ensure a safe operation throughout the testing. Each pilot included a 400 g propane gas bottle connected to a needle valve with an on/off valve and premixed flame burner, connected by a 0.25-in. stainless steel pipe. To confirm the pilot flame during the experiments, a thermocouple was also attached near the pilot flame. This thermocouple was used in the control system with a solenoid valve (normally closed) in the fuel feed line. This solenoid valve remained closed until the pilot flame temperature value exceeded 300 °C, at which the fuel flow to the water seal and flare tip was allowed. This control feature prevented an inadvertent release of fuel to the flare and the surrounding ambient environment.

In addition to the three sections described earlier, the flare system was located below a square aluminum frame section measuring 10 × 10 × 12 ft³ in length, width, and height, respectively. At the top of this frame, a gas hood collected the flare effluent from the flare test. This hood was connected to a draft inducer by a 6-in. diameter duct. An analyzer probe was located at midlength in the exhaust duct to measure combustion efficiency. To ensure accurate measurements and prevent wind effects on the flare flame, two sides of the enclosure were covered with a fiberglass barrier. The third side of the frame was attached to a concrete wall, leaving one side open to access the experiment. Ambient air conditions were measured in the test area before and after each test.

In this study, the combustion emissions analyzer was an Enerac (model 700), that continuously monitored the effluent concentrations of carbon dioxide (CO₂), carbon monoxide (CO), total hydrocarbons (HC), and oxygen (O₂). Also, effluent gas and ambient temperatures were monitored and recorded. An Inconel probe consisting of a 3/8-in. diameter tube, 9-in. as long was used to extract gas samples from the flare effluent. A latex sampling line was used to pass the gas samples from the sampling probe through a thermo-cooler before entering the gas analyzer. The thermo-cooler helped to eliminate moisture from the gas samples before entering the

Table 1. CE for Different Fuel and Air Flow Rates

test ID	fuel flow rate, SLPM	assisted air, SLPM	CE % R1	CE % R2	CE % R3	CE % avg	std deviation (\pm)
A1	5	0	97.428	97.848	97.979	97.752	0.29
A2	5	99.10	95.283	96.838	95.862	95.994	0.79
A3	10	0	98.941	98.872	99.017	98.943	0.07
A4	10	99.10	98.912	99.099	99.037	99.016	0.10
A5	10	141.58	98.921	98.869	98.947	98.912	0.04
A6	10	198.21	95.826	98.565	95.986	96.792	1.54
A7	25	0	99.716	99.660	99.648	99.675	0.04
A8	25	141.58	99.873	99.785	99.811	99.823	0.05
A9	25	198.22	99.541	99.766	99.732	99.680	0.18
A10	25	302.99	99.541	99.486	99.207	99.411	0.18
A11	25	382.28	99.080	99.093	98.656	98.943	0.25
A12	25	467.23	98.654	98.689	97.874	98.406	0.46
A13	120	0	99.805	99.789	99.545	99.713	0.15
A14	120	141.58	99.858	99.874	99.596	99.776	0.16
A15	120	198.22	99.868	99.943	99.602	99.804	0.18
A16	120	302.99	99.861	99.908	99.631	99.800	0.15
A17	120	382.27	99.859	99.863	99.631	99.784	0.13
A18	120	467.23	99.857	99.884	99.613	99.785	0.15
A19	120	566.34	99.870	99.788	99.426	99.695	0.24
A20	120	679.60	99.717	96.700	99.292	98.570	1.63

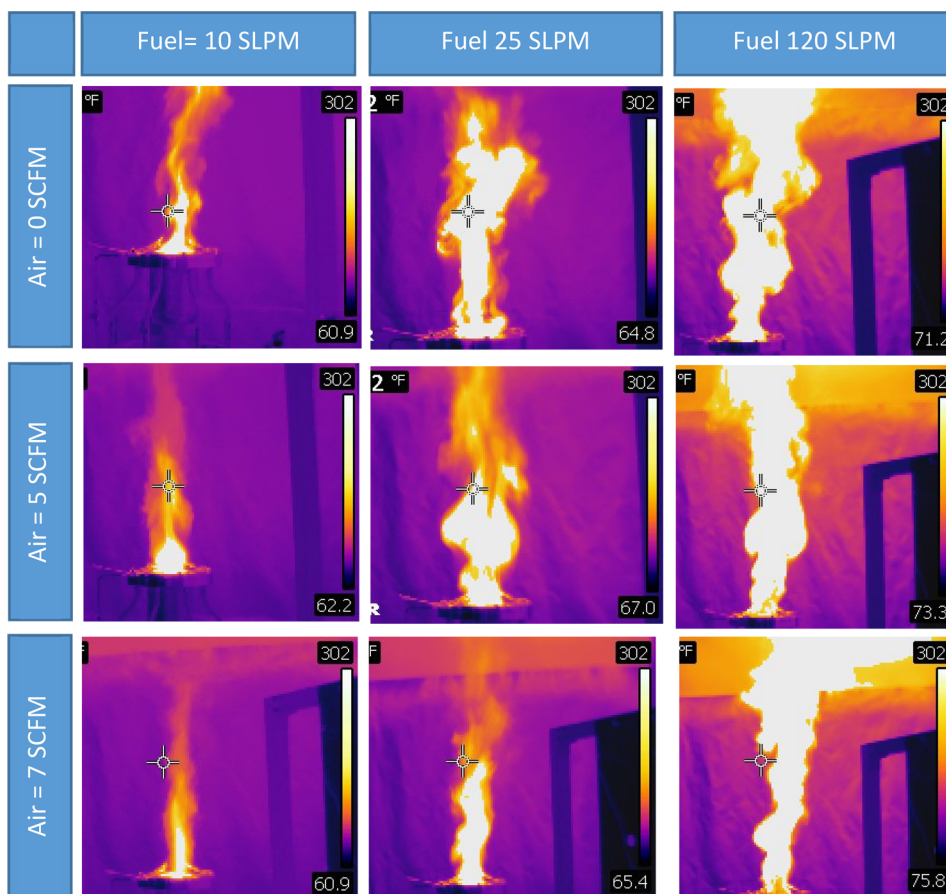


Figure 4. Thermal images of the flame for different fuel and assistant air flow rates.

analyzer which ensured accurate measurements during the test. The analyzer used a built-in pump to draw samples through the sample probe, latex line, and the thermo-cooler to the analyzer. Electrochemical (SEM type), nondispersive-infrared (NDIR), and temperature sensors were used in the analyzer to measure the flare effluent concentrations and temperature. The

analyzer was calibrated by the manufacturer against known concentrations of combustion product gases prior to testing. The accuracies of the analyzer for the measured parameters are 3% for CO, CO₂, and unburned HC each.²⁶

A total of 20 test runs were conducted to assess the new air-assisted flare performance under different operating conditions,

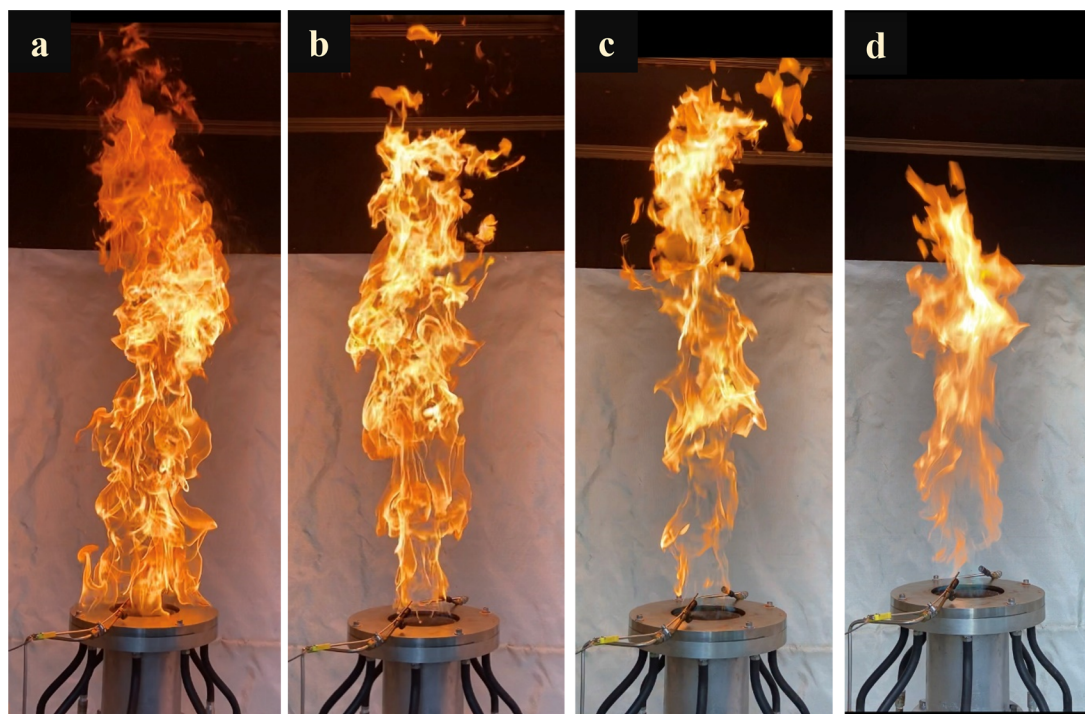


Figure 5. Effects of air jet flow on the flaring flame of 120 SLPM propane with (a) 0 assisted air, (b) 141.58 SLPM, (c) 302.99 SLPM, and (d) 467.23 SPLM.

as summarized in Table 1. Test data reported had units of standard cubic feet per minute (SCFM) and standard liters per minute (SLPM) for the assisted air and flare gas flow rates, respectively.

2.2. Experimental Procedure. The experimental procedure includes the following steps: prior to conducting a new flare test, the water seal was filled with water to the desired level. The second step was to turn on the induced draft fan to clear any combustion products from the flare hood. The pilots were then lighted to provide an ignition source for the flare gas. The mass flow controller software was then initiated and set the flows to the specified values for the flare test. The fuel section was purged using nitrogen through the needle valve to remove any remaining gases completely. The propane gas valve was then opened so it can flow to the flare. The air flow valve was opened and set the flow to the desired value using an air rotameter, so the air can pass through the air distributor and into and out of the radial slot jet. Effluent gas samples through a hood were collected and analyzed using an Enerac (model 700) combustion analyzer for each flare gas flow rate. After conducting the required experiments and taking the related measurements, the propane cylinder valve and the needle valve were closed. To ensure no gas remains in the gas section pipes, these pipes were purged using nitrogen gas. Finally, the nitrogen flow and the air flow to the flare section were shut off, and the pilot flame was shut down by closing the needle valve.

3. RESULTS AND DISCUSSION

In this investigation, an air-assisted flare tip was designed, built, and tested under different operating conditions. A combustion analyzer, Enerac (model 700), was used to measure the concentrations of carbon monoxide, carbon dioxide, and unburned hydrocarbons. Four different fuel flow rates of 5, 10, 25, and 120 SLPM and different amounts of assistant air

flow rates (0–24 SCFM) depending on the fuel flow rates were considered.

3.1. Visual Observation. The thermal images of the flame above the flare tip for different flow rates of fuel and assist air are shown in Figure 4. As can be seen, the flame size increased with increasing the flow rate of the fuel for the same assistant air flow rate. This can be attributed to the higher contact area between fuel gas and air for the diffusion flame above the flare tip. For the same fuel flow rate, increasing the assistant air flow rate causes a reduction in the flame size. Adding more air causes a well-mixed region of fuel and air near the fuel exit. This can burn a larger amount of fuel just after the fuel exits. The stability of the flame increased with the addition of more assisted air flow since the air flow promotes the stability of the flame. When this flare was operated in a nonassisted mode, the flame was indolent and attached to the flare tip. This flame had the highest luminosity created by the excess black carbon created by the flame.

The effect of adding air to the flame above the flare tip for a fuel flow rate of 120 SLPM is shown in Figure 5. For the flame with no air, as shown in Figure 5a, the flame was attached to the tip and the visible region was larger than when using assisted air. The flame also generated a significant amount of visible black soot on the flame edges. This is due to insufficient oxygen in the combustion zone because a flare flame is a diffusion flame that receives the required oxygen by diffusion from the surrounding ambient air. Therefore, this flame generates black soot.⁷ The flame attached to the flare tip can cause microstructural changes in the material of the flare tip as well as high-temperature corrosion, which leads to crack initiation and propagation and ultimately failure.²⁷ As the flow of assistant air increases, black soot is suppressed when assisted air is added to the flame. Also, the flame became more vertical and detached from the flare tip. This was caused by the annular air stream around the flame that was created by the inclined

radial slot jet around the flare tip. This air flow protects the flare tip surface, which gives it a longer lifetime. With higher air flow rates, the flame close to the flare tip becomes blue in color and eventually very light blue color, as shown in Figure 5c and d. This indicates a well-blended mixture of fuel and air.

3.2. Combustion Efficiency. A sample of measured CO₂ and O₂ concentrations and CE % for test A5.R2 is shown in Figure 6. As can be seen, the O₂ concentration values were always less than 19.5 with less than 0.08% deviation. This data is considered to be high-quality measurement.²⁸

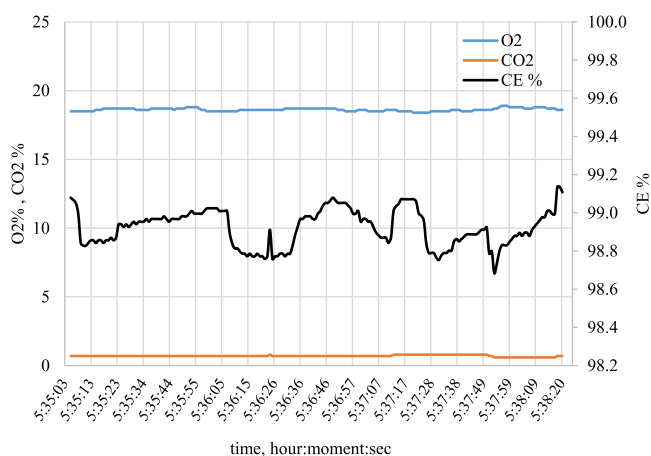


Figure 6. Time series measurement of for CO₂%, O₂% and CE% during air flare tests AS, R2.

The CE for different flow rates with and without assisted medium is shown in Table 1. Table 1 summarizes the operating conditions of the flow rates for the fuel and the assistant air and the results of the test runs for the CE %. The CEs were averaged over a sampling period of 1–4 min. The test runs were replicated three times (labeled as R1, R2, and R3 in Table 1) to ensure the reliability and repeatability of the results and to quantify the error in the measured CE%. Based on the three replications conducted, the standard deviation was estimated for reported CE% values using the equation to estimate standard deviation:

$$S = \left[\frac{\sum_{i=1}^n (CE_i - \overline{CE})^2}{n - 1} \right]^{1/2} \quad (2)$$

where S is the standard deviation, CE_i is the combustion efficiency of run i , \overline{CE} is the average value of the combustion efficiencies of the three runs, which can be calculated from eq 3, and n is the number of replications of each measurement.^{29,30} Also, the average CE is

$$\overline{CE} = \frac{\sum_{i=1}^n X_i}{n} \quad (3)$$

With no air-assisted flow, the CE of the waste gases at flow rates of 5, 10, 20, and 120 SLPM was 97.752, 98.943, 99.675, and 99.713, respectively. At these flow conditions, visible black soot was generated. For each run, when air was added, black soot was eliminated due to increased mixing energy between the waste gas and air, which enhanced the combustion efficiency, as shown in Table 1. One run shown in Table 1 had a CE below 96.5%. This indicates poor flare performance at these high air flow conditions compared to fuel flow rate. This

causes a dilution of the fuel-air mixture in the combustion zone, leading to a nonflammable mixture and lower flare performance. As can also be seen, the combustion efficiency generally increased with the new flare tip.

4. CONCLUSION

The performance of the newly designed flare was assessed by conducting a series of flare tests of the purge flow of waste gases at different operating conditions. Propane gas was used as the flaring gas with four different flow rates of 5, 10, 25, and 120 standard SLPM. Different air-assist flow rate ranges were used within the limits of 3–18 SCFM of air flow rate. Combustion efficiencies were calculated by using the species concentration measurements of extracted samples from the plume. The findings demonstrated that at low flow rates, waste gases can cause significant visible soot formation. However, the results also showed that injection air from the radial slot around the flare tip suppressed soot formation and enhanced the combustion efficiency. Another finding of this study was that combustion efficiency was generally above 96.5% but there was soot formation in the plume, which means that soot formation does not impact combustion efficiency. Because of the well mixing region between the fuel gas and injected air, a blue or very light blue color flame was generated near the flare tip. The new flare tip design has protected the flare tip by forming an annular air stream around the fuel, which causes flame stability away from the flare tip. The results also demonstrated the effectiveness of the new design in flaring gases with high combustion efficiency and smokeless operation.

■ ASSOCIATED CONTENT

SI Supporting Information

The Supporting Information is available free of charge at <https://pubs.acs.org/doi/10.1021/acsomega.2c04618>.

Brief review of the previous studies related to the flare testing under different operating parameters (PDF)

■ AUTHOR INFORMATION

Corresponding Author

Joseph D. Smith – Chemical and Biochemical Engineering, Missouri University of Science and Technology, Rolla, Missouri 65409-1230, United States; orcid.org/0000-0002-1778-6156; Email: smithjose@mst.edu

Authors

Hayder A. Alhameedi – Chemical and Biochemical Engineering, Missouri University of Science and Technology, Rolla, Missouri 65409-1230, United States; Chemical Engineering, College of Engineering, University of AL-Qadisiyah, Al-Diwaniyah 58001, Iraq; orcid.org/0000-0002-0900-0942

Paul Ani – Chemical and Biochemical Engineering, Missouri University of Science and Technology, Rolla, Missouri 65409-1230, United States

Tanner Powley – Chemical and Biochemical Engineering, Missouri University of Science and Technology, Rolla, Missouri 65409-1230, United States

Complete contact information is available at: <https://pubs.acs.org/doi/10.1021/acsomega.2c04618>

Notes

The authors declare no competing financial interest.

ACKNOWLEDGMENTS

The authors would like to express their gratitude to the Higher Committee for Education Development of Iraq (HCED), Ministry of Higher Education and Scientific Research (Iraq) for their financial support. The authors also gratefully acknowledge the financial support of the Wayne and Gayle Laufer Foundation. The authors also would like to thank Mrs. Eileen Smith for her editorial assistance in the preparation of the manuscript.

REFERENCES

- (1) Smith, J. D.; Al-Hameedi, H.; Jackson, R.; Suo-Antilla, A. Testing and Prediction of Flare Emissions Created during Transient Flare Ignition. *Journal of Petrochemistry and Research* **2018**, *2* (2), 175–181.
- (2) Yu, P.; Xu, R.; Coelho, M. S.; Saldiva, P. H.; Li, S.; Zhao, Q.; Mahal, A.; Sim, M.; Abramson, M. J.; Guo, Y. The impacts of long-term exposure to PM_{2.5} on cancer hospitalizations in Brazil. *Environ. Int.* **2021**, *154*, 106671.
- (3) Pavlovic, R. T.; Al-Fadhli, F. M.; Kimura, Y.; Allen, D. T.; McDonald-Buller, E. C. Impacts of Emission Variability and Flare Combustion Efficiency on Ozone Formation in the Houston–Galveston–Brazoria Area. *Ind. Eng. Chem. Res.* **2012**, *51*, 12593–12599.
- (4) Enforcement-Alert. *EPA Enforcement Targets Flaring Efficiency Violations*. EPA 325-F-012-002, 2012.
- (5) Baukal, C.; Schwartz, R. *The John Zink Combustion Handbook*; CRC Press: New York, 2001.
- (6) TCEQ 2010 Flare Study Final Report, The University of Texas at Austin, The Center for Energy and Environmental Resources, TCEQ PGA No. 582-8-86245-FY09-04 and Task Order No. UTA10-000924-LOAT-RP9, Aug. 1, 2011.
- (7) Castineira, D.; Edgar, T. CFD for Simulation of Steam-Assisted and Air-Assisted Flare Combustion Systems. *Energy Fuels* **2006**, *20* (3), 1044–1056.
- (8) Alhameedi, H. A.; Hassan, A. A.; Smith, J. D.; Al-Dahhan, M. Toward a Better Air-Assisted Flare Design for Purge Flow Conditions: Experimental and Computational Investigation of Radial Slot Flow into a Crossflow Environment. *Ind. Eng. Chem. Res.* **2021**, *60* (6), 2634–2641.
- (9) McDaniel, M. *Flare Efficiency Study*; United States Environmental Protection Agency: Washington, DC; Report No. 600/2-83-052, July 1983.
- (10) Pohl, J. H.; Soelberg, N. R. *Evaluation of the Efficiency of Industrial Flares: Flare Head Design and Gas Composition*; United States Environmental Protection Agency: Research Triangle Park, NC; Report No. EPA-600/2-85-106, January 1986.
- (11) Ahsan, A.; Ahsan, H.; Olfert, J. S.; Kostiuik, L. W. Quantifying the carbon conversion efficiency and emission indices of a lab-scale natural gas flare with internal coflows of air or steam. *Experimental Thermal and Fluid Science* **2019**, *103*, 133–142.
- (12) Bello, O. W.; Zamani, M.; Abbasi-Atibeh, E.; Kostiuik, L. W.; Olfert, J. S. Comparison of emissions from steam- and water-assisted lab-scale flames. *Fuel* **2021**, *302*, 121107.
- (13) Singh, K. D.; Gangadharan, P.; Chen, D. H.; Lou, H. H.; Li, X.; Richmond, P. Computational Fluid Dynamics Modeling of Laboratory Flames and an Industrial Flare. *Journal of the Air & Waste Management Association*. **2014**, *64*, 1328–1340.
- (14) Singh, K. D.; Dabade, T.; Vaid, H.; Gangadharan, P.; Chen, D. H.; Lou, H. H.; Li, X.; Li, K.; Martin, C. B. Computational Fluid Dynamics Modeling of Industrial Flares Operated in Stand-By Mode. *Ind. Eng. Chem. Res.* **2012**, *51*, 12611–12620.
- (15) Pohl, J. H.; Payne, R.; Lee, J. *Evaluation of the Efficiency of Industrial Flares: Test Results*; United States Environmental Protection Agency: Research Triangle Park, NC; Report No. EPA-600/2-84-095, NC, May 1984.
- (16) Castiñeira, D.; Edgar, T. CFD for Simulation of Crosswind on the Efficiency of High Momentum Jet Turbulent Combustion Flames. *J. Environ. Eng.* **2008**, *134* (7), 561–571.
- (17) Castiñeira, D.; Edgar, T. Computational Fluid Dynamics for Simulation of Wind-Tunnel Experiments on Flare Combustion Systems. *Energy Fuels* **2008**, *22*, 1698–1706.
- (18) Zamani, M.; Abbasi-Atibeh, E.; Mobaseri, S.; Ahsan, H.; Ahsan, A.; Olfert, J. S.; Kostiuik, L. W. An experimental study on the carbon conversion efficiency and emission indices of air and steam co-flow diffusion jet flames. *Fuel* **2021**, *287*, 119534.
- (19) Torres, V. M.; Herndon, S.; Allen, D. T. Industrial Flare Performance at Low Flow Conditions. 2. Steam- and Air-Assisted Flares. *Ind. Eng. Chem. Res.* **2012**, *51* (39), 12569–12576.
- (20) Torres, V. M.; Herndon, S.; Wood, E.; Al-Fadhli, F. M.; Allen, D. T. Emissions of Nitrogen Oxides from Flares Operating at Low Flow Conditions. *Ind. Eng. Chem. Res.* **2012**, *51* (39), 12600–12605.
- (21) Torres, V. M.; Herndon, S.; Kodesh, Z.; Allen, D. T. Industrial Flare Performance at Low Flow Conditions. 1. Study Overview. *Ind. Eng. Chem. Res.* **2012**, *51* (39), 12559–12568.
- (22) Smith, S.; Seefeldt, G. *Use of Variable Frequency Drives for Better Destruction Efficiency of Air-Assisted Flares*; American Flame Research Committee, Kauai, HI, 2013.
- (23) Al-Fadhli, F. M.; Torres, V. M.; Allen, D. T. Impacts of Air-Assist Flare Blower Configurations on Flaring Emissions. *Ind. Eng. Chem. Res.* **2012**, *51* (39), 12606–12610.
- (24) Mostafayi, S. S.; Rashidi, F. Effect of dividing single flare tip into multiple tips on soot reduction. *Clean Technologies and Environmental Policy* **2020**, *22*, 1097–1108.
- (25) Alhameedi, H. A.; Hassan, A. A.; Smith, J. D. Towards a better air assisted flare design for low flow conditions: Analysis of radial slot and flow effects. *Process Safety and Environmental Protection* **2022**, *157*, 484–492.
- (26) Enerac. Instruction Manual Integrated Emissions System Model 700. *ENERAC 700 MANUAL*; ENERAC, LLC: Holbrook, NY, 2018.
- (27) Al-Shaikhali, A. H.; Al-Badairy, H. H.; El-Sherik, A. M. Smokeless flare tips failure investigation: case study. *Materials at High Temperatures* **2020**, *37* (1), 11–15.
- (28) Zeng, Y.; Morris, J.; Dombrowski, M. Validation of new method for measuring and continuously monitoring the efficiency of industrial flares. *J. Air Waste Manage. Assoc.* **2016**, *66* (1), 76–86.
- (29) Callister, W. D. *Fundamentals of Materials Science and Engineering: An interactive e.text*; John Wiley and Sons: New York, 2001.
- (30) Burr, D. C.; Corbin, D. J.; Armitage, J. R.; Crosland, B. M.; Jefferson, A. M.; Kopp, G. A.; Kostiuik, L. W.; Johnson, M. R. A methodology for quantifying combustion efficiencies and species emission rates of flares subjected to crosswind. *Journal of the Energy Institute* **2022**, *104*, 124–132.